Hindawi
Shock and Vibration
Volume 2023, Article ID 6621439, 14 pages
https://doi.org/10.1155/2023/6621439

Research Article

Investigations of Dynamic Mechanical Performance of Rubber Concrete under Freeze-Thaw Cycle Damage

Jingli Zhang

College of Civil Engineering, Zhengzhou University of Science and Technology, Zhengzhou Henan 450064, China

Correspondence should be addressed to Jingli Zhang; zhangjingli@zit.edu.cn

Received 4 May 2023; Revised 18 September 2023; Accepted 27 September 2023; Published 25 October 2023

Academic Editor: Andrea Spaggiari

In order to study the effect of the freeze-thaw cycle on the integrity and dynamic mechanical performance of rubber concrete, the wave speed of rubber concrete specimens with 10% rubber volume was measured by a nonmetallic ultrasonic detector. The impact tests were also performed on rubber concrete specimens with different numbers of freeze-thaw cycles (0, 25, 50, 75, 100, and 125) at different impact air pressures (0.3, 0.4, 0.5, and 0.6 MPa) using a 74 mm diameter split Hopkinson pressure bar (SHPB) device, peak stress, ultimate strain dynamic intensity enhancement factor (DIF), and energy absorption effect. The results show that with the increase of freeze-thaw cycles, the wave speed decreases, and the freeze-thaw action will damage the rubber concrete and reduce the longitudinal wave velocity. Under the same freeze-thaw cycles, with the rise of strain rate, the peak stress, limit strain, DIF, and absorbed energy increase, and there is an obvious strain rate effect; under the pressure of 0.6 MPa, the peak stress of 25, 50, 75, 100, and 125 freeze-thaw cycles decreases by 25.1%, 37.1%, 46%, 52.5%, and 54.8%. With the increase of the freeze-thaw cycles, the peak stress of the specimen decreases, and the decrease gradually decreases. After the number of cycles exceeds 100, the stress decrease of the specimen is no longer obvious, the limit strain increases, and the absorbed energy decreases. The freeze-thaw environment significantly reduces the strength and integrity of rubber concrete specimens.

1. Introduction

The annual production of waste rubber products is huge worldwide, and if they are directly disposed of in landfills and incinerators, it will not only cause waste of resources but also cause environmental pollution. Therefore, the reuse of waste rubber materials is important for the protection of resources and the environment [1–3]. At present, the domestic construction industry advocates energy saving, environmental protection, and green development, and research has shown that mixing a certain amount of rubber particles into concrete can effectively improve its mechanical performance [4]. Hu et al. [5] found that as the amount of rubber admixture increased, the compressive, tensile, and shear strengths of the specimens subsequently decreased and the ductility increased. Son et al. [6] found that the incorporation of rubber in concrete reduces its compressive strength and modulus of elasticity, but its deformation and absorption energy increases, and its curvature ductility increases by nearly 90%. Zhao et al. [7] carried out dynamic compression tests on rubber concrete using the SHPB test apparatus and found that its damage level was significantly lower than ordinary concrete and its energy dissipation capacity was significantly higher.

The northeast and northwest of China are in the monsoon freeze zone, and concrete buildings are in the freeze-thaw environment [8]. It has been shown that freeze-thaw cycling changes the internal structure of the specimen, thus changing its mechanical properties. Zhou et al. [9, 10] studied the uniaxial compressive mechanical properties of fractured sandstone under freeze-thaw fatigue damage. The results indicate that freeze-thaw cycles can cause fatigue damage to the specimen, leading to new microcracks and micropores, thereby reducing the mechanical properties of the specimen. Tian et al. [11] studied the deterioration mechanism of concrete, and the tests showed that the elastic modulus and strength decreased significantly with the increase of the freeze-thaw. Cao et al. [12] found that the peak

strain of concrete specimens increased with the increase of the freeze-thaw effect. Zhou et al. [13] found that freeze-thaw cycles reduce the ultimate compressive strength of steel fiber concrete and the rate of decline increases significantly after 100 freeze-thaw actions. Wang et al. [14] found that the strengths of recycled concrete under freeze-thaw cycles were subsequently reduced, and their deterioration was higher than that of ordinary concrete. Fan et al. [15] found that the compressive and flexural properties all decreased with the action of the freeze-thaw effect. Freeze-thaw cycles can cause damage to rubber concrete and reduce its mechanical performance. However, the present research results only stay under static load, and there is little research on the mechanical performance of rubber concrete under dynamic load after freeze-thaw cycles. Concrete materials are often subjected to dynamic loads such as impacts and vibrations during their design service life and their mechanical performance under dynamic loads differ in many ways from those under static loads [16].

To further study the mechanical performance of rubber concrete under dynamic load after freeze-thaw cycles, a sonic detector was used to measure the degree of damage to rubber concrete under freeze-thaw times. The uniaxial impact compression test of freeze-thaw rubber concrete was carried out by using φ74 mm SHPB device to analyze the influence law of the freeze-thaw cycles and strain rate on the longitudinal wave velocity, peak stress, ultimate strain, and energy absorption effect of rubber concrete, so as to provide a test basis for rubber concrete engineering.

2. Program

2.1. Materials. The test uses P·O 42.5 cement, the fine aggregate is sand, the coarse aggregate uses the particle size less than 18 mm gravel, and tap water. The selected rubber particles have a particle size range of 1~3 mm, as shown in Figure 1.

It was shown that the best volume dosage of rubber granules in rubber concrete is 10%, and the design strength of the base concrete was 30 MPa [17]. Rubber replaces sand by 10% of equal volume, and the mass ratio is cement : sand : rubber : water : stone = 1 : 1.125 : 0.052 : 0.4 : 2.3 after the specimen is poured and placed under standard maintenance conditions for maintenance. After maintenance, the specimens will be processed into $\varphi 50 \times 100$ mm and $\varphi 74 \times 37$ mm cylindrical standard specimens by taking the core, cutting, and grinding, with 3 specimens in each group. A total of 18 rubber concrete specimens were tested in a static compression test, and 72 specimens were tested in a dynamic compression test. The nonparallelism of both end surfaces of the specimens was less than 0.05 mm, and the flatness of one side was within 0.02 mm [18].

Figure 1: Selection of rubber particles.

2.2. Test Equipment and Method. The freeze-thaw cycles are 0, 25, 50, 75, 100, and 125 times, respectively. During the freeze-thaw cycle, the minimum temperature in the center of the specimen was controlled at $(-18 \pm 2)^{\circ}$C and the maximum temperature was controlled at $(5 \pm 2)^{\circ}$C. A group of specimens was selected for ultrasonic testing immediately. The compression test was carried out immediately after the freeze-thaw cycle. Uniaxial compression tests were conducted to obtain macroscopic mechanical indices. A 74 mm diameter SHPB test apparatus was used to get dynamic compression tests. The structure of the test setup is shown in Figure 2.

The dynamic test was carried out by the impact dynamics laboratory φ74 mm variable section SHPB test device, using different impact air pressures (0.3, 0.4, 0.5, and 0.6 MPa) on the specimen. The bullet acquires a velocity v under the impact air pressure to strike the incident bar, and an incident wave is formed by the pulsing of the incident bar. When the wave reaches the contact surface between the end of the incident rod and the specimen, part of the pulse is reflected back to form a reflected wave, and the other part is transmitted to form a transmitted wave in the transmission rod. The pulse signals are collected and displayed by an oscilloscope, whose wave forms are shown in Figure 3. In order to ensure the validity of the impact test data, stress balance testing is required for each impact data. The stress balance is shown in Figure 4 [19].

The collected data are solved by applying the corresponding calculation formulae, some of which are described in the following [20, 21]:

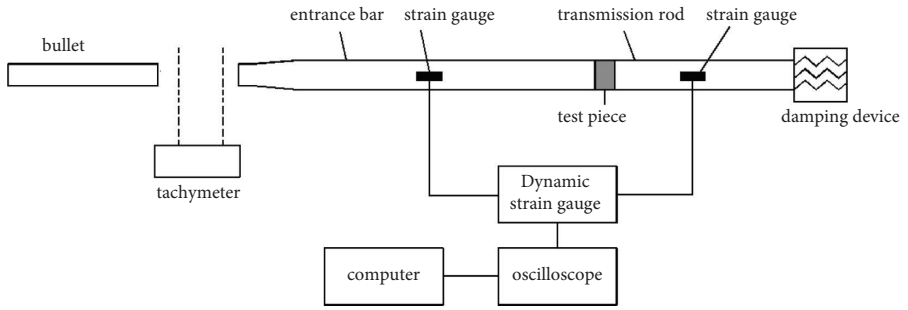

Figure 2: Schematic diagram of SHPB device.

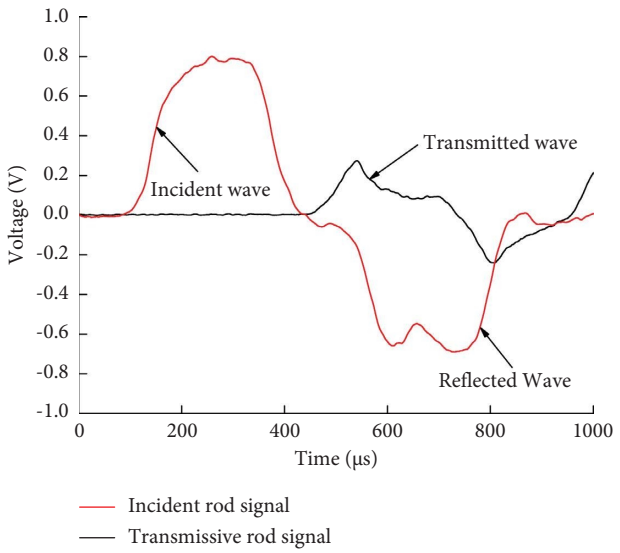

Figure 3: Measured waveform.

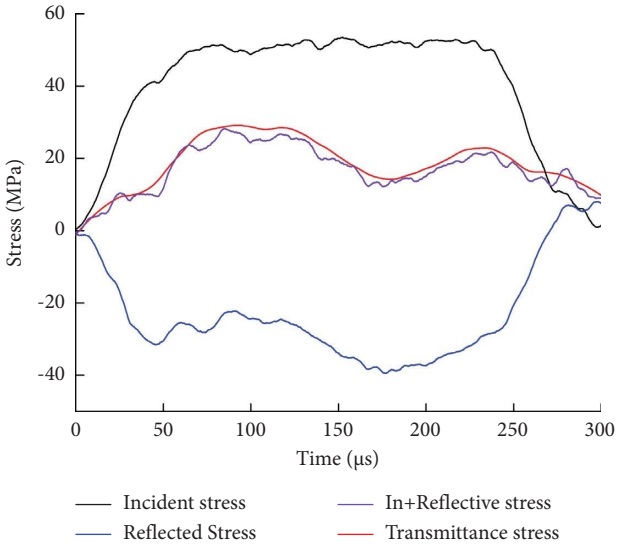

Figure 4: Stress equilibrium curve.

$$\begin{cases} \dot{\varepsilon}(t) = \dfrac{C_0}{l_s}\left[\varepsilon_i(t) - \varepsilon_r(t) - \varepsilon_t(t)\right], \\ \varepsilon(t) = \dfrac{C_0}{l}\displaystyle\int_0^t \left[\varepsilon_i(t) - \varepsilon_r(t) - \varepsilon_t(t)\right]\mathrm{d}t, \\ \sigma(t) = \dfrac{AE}{2A_S}\left[\varepsilon_i(t) + \varepsilon_r(t) + \varepsilon_t(t)\right], \end{cases} \tag{1}$$

$$\begin{cases} W_i(t) = AEC_0\displaystyle\int_0^t \varepsilon_i^{\,2}(t)\mathrm{d}t, \\ W_r(t) = AEC_0\displaystyle\int_0^t \varepsilon_r^{\,2}(t)\mathrm{d}t, \\ W_t(t) = AEC_0\displaystyle\int_0^t \varepsilon_t^{\,2}(t)\mathrm{d}t. \end{cases}$$

$$W_s(t) = W_i(t) - W_r(t) - W_t(t), \tag{2}$$

$$\varepsilon_d = \frac{W_s(t)}{V}, \tag{3}$$

where W_i is the incident energy, J; W_t is the transmitted energy, J; W_r is the reflected energy, J; W_s is the energy absorbed, J; C_0 is the longitudinal wave speed in the compressional rod, m/s; ε_d is the unit absorbed energy density, J. cm^{-3}; and V is the volume, cm^3.

3. Results

3.1. Comparison of Mechanical Performance of Two Concrete Materials. In order to analyze the mechanical performance of plain concrete and rubber concrete under dynamic load when the rubber substitution rate is 10%, quasi-static compression and dynamic impact tests were conducted on two types of specimens with the same ratio, and the results are shown in Table 1. The stress-strain curves of plain concrete and rubber concrete at different average strain rates (whose values are the average values of the stable section of

Table 1: Mechanical performance of two concrete materials.

Number	Average strain rate (s^{-1})	Dynamic strength (MPa)	Toughness (J)	Static average compressive strength (MPa)	W_i (J)	W_s (J)	Energy absorption rate (%)	ε_d ($J \cdot cm^{-3}$)
XJ-0-0.3	75.1	40.1	0.43	34.2	63.2	18.6	29.5	0.12
XJ-0-0.4	99.8	46.8	0.66		85.4	26.7	31.3	0.17
XJ-0-0.5	127.2	60.2	0.80		106.7	36.1	33.8	0.23
XJ-0-0.6	155.9	74.5	1.17		146.8	47.6	32.4	0.30
XJ-10-0.3	72.3	37.5	0.60	31.5	60.3	24.7	41.0	0.16
XJ-10-0.4	96.7	45.7	0.79		79.5	33.8	42.5	0.22
XJ-10-0.5	124.6	57.3	1.05		103.2	49.7	48.2	0.32
XJ-10-0.6	151.7	70.6	1.33		141.7	61.6	43.4	0.38

Note. XJ-10-0.3 in XJ indicates rubber concrete, 10 indicates rubber admixture of 10%, 0.3 indicates impact air pressure of 0.3 MPa.

the reflected waves) are shown in Figures 5 and 6, the change in toughness is shown in Figure 7, and the density of absorbed energy per unit is shown in Figure 8.

From Table 1, Figures 5, and 6, it can be seen that the peak stresses in plain concrete are overall higher than those in rubber concrete at different impact air pressures, which shows consistency with the results of numerous studies [5, 6]. However, rubber concrete is significantly more ductile than plain concrete and has a higher deformation capacity. Toughness refers to the ability of a material to deform under external load and is a reflection of the comprehensive performance of material ductility and strength, which can be expressed using the area enclosed between the stress-strain curve and the coordinate axis of the specimen under external load [22]. As can be seen from Figure 7, the toughness of rubber concrete is significantly higher than that of plain concrete, which can effectively prevent the building from brittle damage under external load.

To further study the energy absorption effect of rubber concrete, the energy change under different impact air pressures was analyzed, and the results are shown in Table 1 and Figure 8. With the rise of pressure, the incident and absorbed energy increased, and the energy absorption rate of rubber concrete was significantly higher than that of plain concrete. Figure 8 shows that with the rise of air pressure, the density of absorbed energy per unit increases, and the density of absorbed energy of rubber concrete is significantly higher than that of plain concrete, and the incorporation of rubber can effectively enhance the energy absorption effect of concrete materials. Rubber as an elastic material can increase the plastic deformation capacity of concrete. Rubberized concrete specimens in the external load after the external part of the energy will be stored in the way of elastic energy in the rubber particles, which greatly enhances the specimen's energy consumption effect. At the same time, the incorporation of rubber particles can also improve the bonding characteristics between the cementitious material and the aggregate, which also greatly improves the ductility of the specimen.

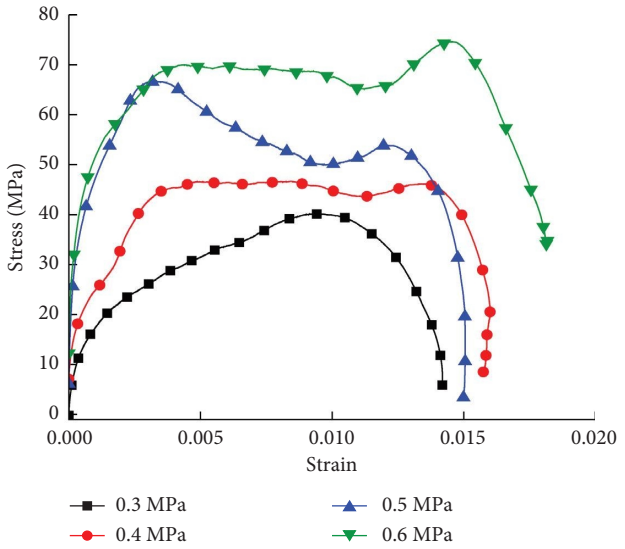

Figure 5: Stress-strain curves of plain concrete.

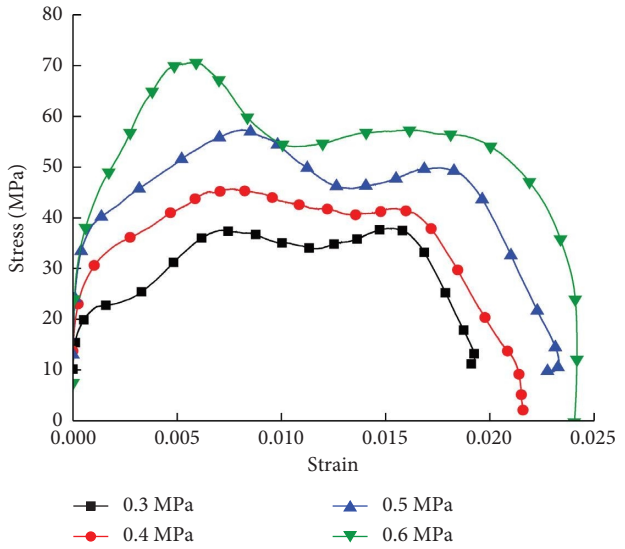

Figure 6: Stress-strain curves of rubber concrete.

3.2. Ultrasonic Testing of Specimens under Freeze-Thaw Cycles. The internal integrity of the material can be measured by the ultrasonic inspection principle [23]. There are cracks and pores inside the concrete material, and the elastic wave propagation inside the material will reflect, refract, and bypass when it encounters the cracks. The macroscopic expression is the increase of the elastic wave propagation path and the decrease of the wave speed. The wave speed of

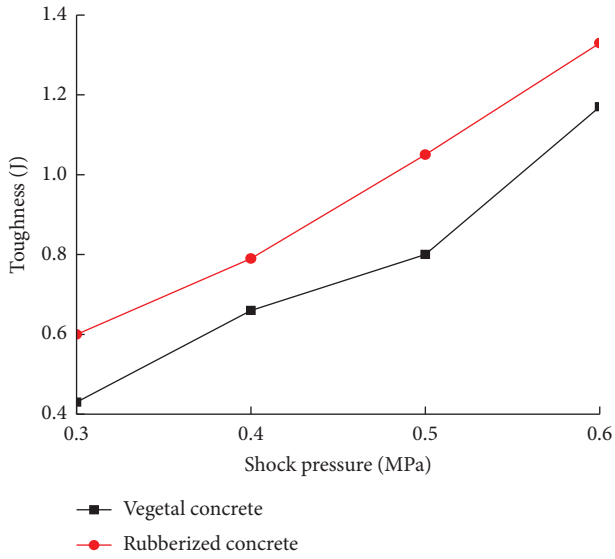

Figure 7: Toughness of specimens under different impact pressure.

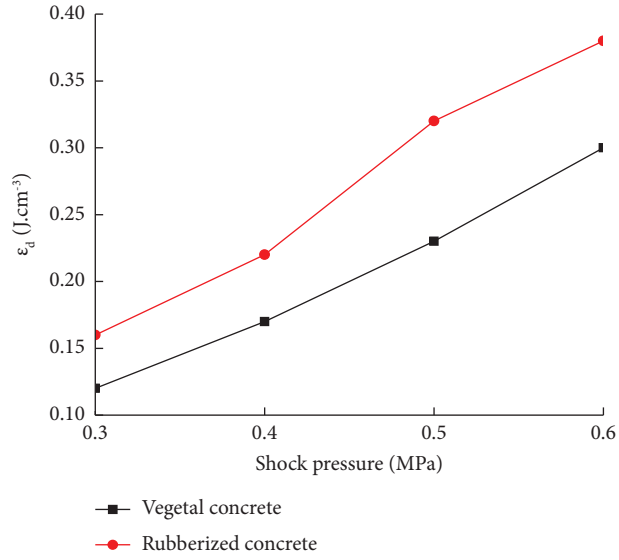

Figure 8: Unit absorbed energy density of specimen under different impact pressure.

rubber concrete was measured at the end of the freeze-thaw cycles, and the damage degree was calculated under freeze-thaw cycles, and the test results are shown in Table 2, Figures 9, and 10.

As shown in Table 2 and Figure 9, with the rise of freeze-thaw cycles, the longitudinal wave velocity of rubber concrete specimens tends to decrease. Compared with the unfreeze-thaw specimens, the longitudinal wave velocity of specimens with 25 freeze-thaw cycles decreases by 9.5%, 16.1% at 50 cycles, and 23.4% and 24.7% at 100 and 125 cycles, respectively.

To further evaluate the internal damage of the rubber concrete specimens after freezing cycles, the damage degree was defined as D, which is calculated as shown in (2) [24], and the damage degree under different numbers of freeze-thaw cycles is shown in Figure 10.

$$D = 1 - \frac{V_T}{V_0}, \tag{4}$$

where D is the degree of damage; V_T is the wave speed after the freeze-thaw cycle, m/s; and V_0 is the wave speed without freeze-thaw cycle, m/s.

Figure 10 shows that with the rise of freeze-thaw cycles, the degree of rubber concrete damage increases, and the increase gradually decreases, which shows consistency with the law of change of the wave speed. Analysis of the reason: there is a large amount of pore water inside the rubber concrete specimen, and research shows that the pore water will produce about 9% volume expansion due to freezing [25], causing the expansion of the native pores inside the concrete, while the expansion of the water volume will produce stress inside the specimen, causing the expansion of

Table 2: Longitudinal wave velocity of specimen under freeze-thaw cycle.

Number	Specimen height L (mm)	Initial sound time value (μs)	Measured sound time value (μs)	Wave speed (m·s^{-1})	Average (m·s^{-1})	D
XJ-0-1	99.8	3.2	31.8	3490		
XJ-0-2	100.3	3.2	31.4	3557	3552	0
XJ-0-3	100.3	3.2	31.0	3608		
XJ-25-1	99.73	3.2	34.8	3156		
XJ-25-2	101.14	3.2	34.0	3284	3215	0.095
XJ-25-3	99.13	3.2	34.2	3204		
XJ-50-1	100.59	3.2	37.0	2891		
XJ-50-2	98.74	3.2	36.8	2939	2979	0.161
XJ-50-3	100.06	3.2	35.4	3107		
XJ-75-1	99.37	3.2	37.8	2872		
XJ-75-2	98.89	3.2	38.4	2809	2826	0.204
XJ-75-3	100.42	3.2	39.2	2798		
XJ-100-1	99.26	3.2	39.2	2757		
XJ-100-2	99.42	3.2	39.8	2716	2722	0.234
XJ-100-3	100.21	3.2	40.4	2694		
XJ-125-1	99.46	3.2	38.6	2710		
XJ-125-2	99.42	3.2	40.4	2673	2673	0.247
XJ-125-3	101.21	3.2	41.6	2636		

Note. XJ-0-1 in XJ means rubber concrete, 0 means the number of freeze-thaw cycles is 0, 1 means the test piece number is 1.

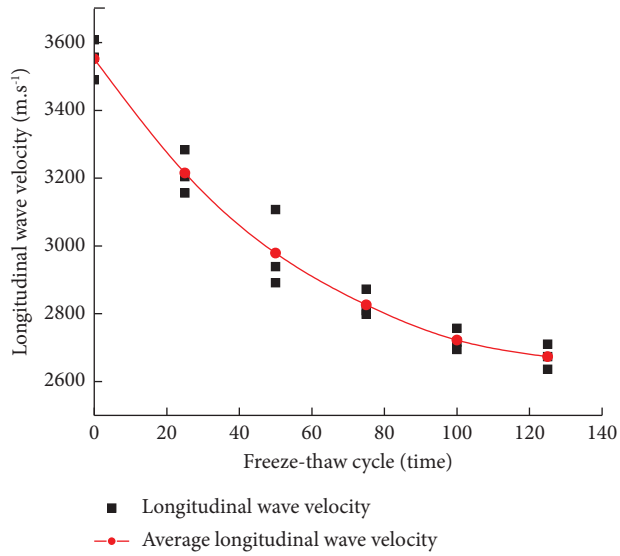

Figure 9: Relationship between freeze-thaw cycle times and longitudinal wave velocity.

the internal cracks. In the process of alternating positive and negative temperature will generate a certain tensile stress, so that the rubber concrete produces fatigue damage, and under the repeated action of freeze-thaw cycles, the internal pore cracks expand and the damage degree increases [26]. When the wave propagates inside the specimen, reflection and bypassing will occur when it encounters pore cracks, making the wave speed decrease. Longitudinal wave velocity and damage reduction amplitude gradually decreased, which is due to the repeated expansion of pore water to increase the porosity, the late freeze-thaw effect on the internal structure of concrete reduced, the amount of new pores subsequently reduced, and the longitudinal wave velocity reduction amplitude and damage increase decreased.

3.3. Stress-Strain Curve. The three-wave method was used to process the data collected from the specimens, and the test results are shown in Table 3. The stress-strain curves of rubber concrete under static load are shown in Figure 11. The average strain rates obtained under different pressures are shown in Figure 12, and the stress-strain curves of freeze-thaw cycles under 0.4 MPa are shown in Figure 13.

Due to the existence of a large number of primary cracks inside the concrete material, the stress-strain curve under static load includes four stages: pore compacting, elasticity, yielding, and damage. Unlike the static load action, the stress-strain curve under dynamic load includes three stages: elasticity, yield, and damage. Under the action of a high strain rate, the specimen is subjected to the load for a very

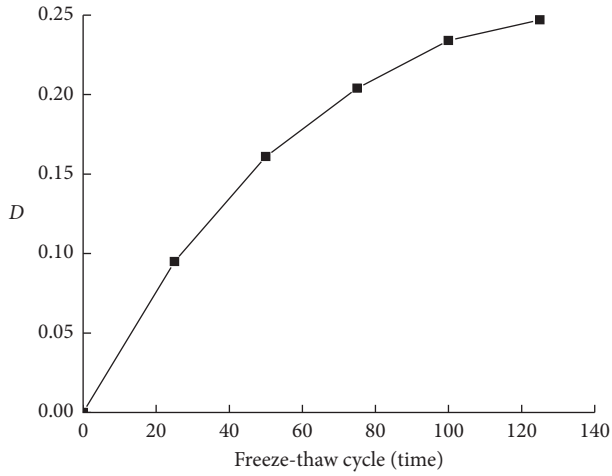

Figure 10: Relationship between freeze-thaw cycle times and damage degree.

Table 3: Test results of rubber concrete under freeze-thaw cycle.

Number	Average strain rate (s^{-1})	Specimen height (mm)	Diameter (mm)	Dynamic compressive strength (MPa)	Dynamic ultimate strain (10^{-3})	Static average strength (MPa)	DIF	Absorption energy (J)
XJ-0-0.3	72.3	36.98	74.12	37.5	19.8	31.5	1.19	24.7
XJ-0-0.4	96.7	37.02	73.56	45.7	21.6		1.45	33.8
XJ-0-0.5	124.6	36.38	73.98	57.3	23.3		1.82	49.7
XJ-0-0.6	151.7	37.72	74.00	70.6	24.1		2.24	61.6
XJ-25-0.3	78.1	37.78	73.78	31.2	21.5	25.8	1.21	19.5
XJ-25-0.4	99.6	37.01	73.78	36.4	22.5		1.41	28.4
XJ-25-0.5	127.1	36.02	73.97	44.1	24.1		1.71	40.6
XJ-25-0.6	155.4	37.18	73.89	52.9	24.6		2.05	53.5
XJ-50-0.3	74.6	36.78	74.34	25.8	22.1	22.4	1.15	18.6
XJ-50-0.4	102.6	37.16	74.21	31.6	23.1		1.41	26.7
XJ-50-0.5	128.7	37.32	73.42	36.3	24.8		1.62	37.8
XJ-50-0.6	156.3	37.67	74.22	44.4	25.7		1.98	52.1
XJ-75-0.3	77.4	36.76	73.98	24.2	22.6	20.7	1.17	16.7
XJ-75-0.4	99.2	36.59	73.78	27.9	23.9		1.35	28.3
XJ-75-0.5	130.9	37.18	74.57	34.0	25.5		1.64	33.8
XJ-75-0.6	154.3	37.38	74.25	38.1	26.7		1.84	49.3
XJ-100-0.3	73.2	37.25	74.06	22.3	22.5	18.6	1.20	14.1
XJ-100-0.4	95.6	36.87	74.10	25.7	24.8		1.38	23.6
XJ-100-0.5	133.5	36.77	74.02	29.8	26.1		1.60	29.5
XJ-100-0.6	158.2	36.85	74.06	33.5	27.5		1.80	40.2
XJ-125-0.3	74.4	37.08	73.95	21.7	23.3	17.9	1.21	15.3
XJ-125-0.4	98.2	37.42	73.92	27.4	25.5		1.53	25.1
XJ-125-0.5	129.6	37.30	74.11	29.2	26.7		1.63	28.9
XJ-125-0.6	157.7	37.05	74.15	31.9	27.9		1.78	35.7

Note. XJ-0-0.3 in XJ means rubber concrete, 0 means the number of freeze-thaw cycles is 0, 0.3 means the air pressure is 0.3 MPa.

short time, the specimen internal primary pore cracks cannot be compressed directly into the elastic deformation phase, the curve in this phase is approximately a straight line up, the slope of the curve is close to a constant value, the constant value can be used as the dynamic elastic modulus. Figure 12 shows that as the air pressure increases, the average strain rate increases, and there is a linear positive correlation between the two. Figure 13 shows that with the rise of the freeze-thaw cycles, the peak stress of the rubber concrete specimen decreases, the drop rate gradually decreases, and the ultimate strain increases. When the number of freeze-thaw cycles exceeds 75, the change in peak stress in the specimen will no longer be significant. This is due to the freezing effect and alternating temperature differences in the internal stress, the specimen internal pore crack expansion, in the cementitious material and aggregate, rubber contact surface to produce new cracks, while the rubber in repeated freeze-thaw damage will also occur, resulting in damage to the specimen, the stress is then reduced. With the rise of freeze-thaw cycles, the freezing effect

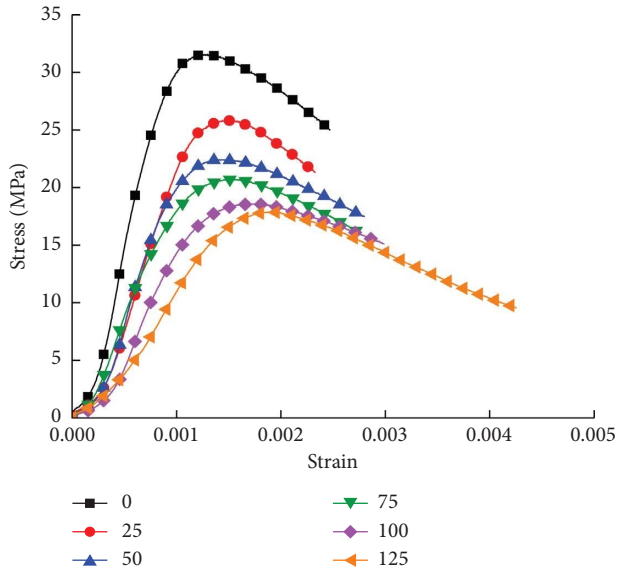

Figure 11: Stress-strain curve under static load.

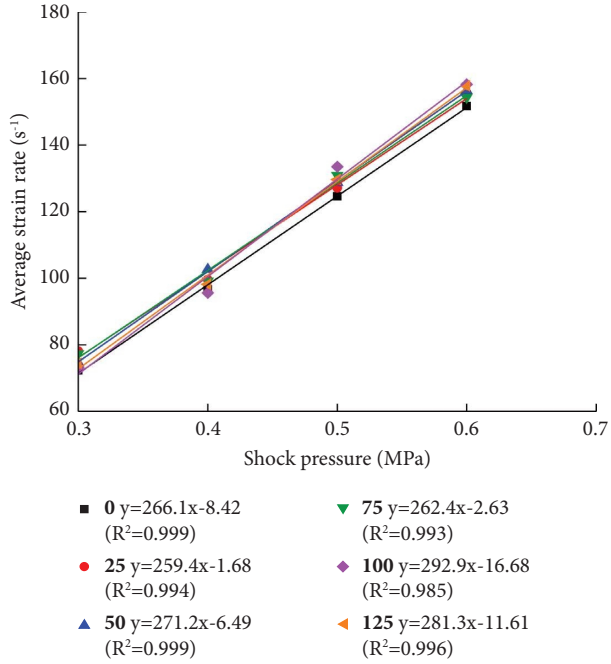

Figure 12: Relationship between pressure and strain rate.

will no longer be obvious, and the incremental damage to the specimen will be reduced.

3.4. Peak Stress and Absorbed Energy. The peak stresses of freeze-thaw cycled rubber concrete at different impact air pressures are shown in Figure 14, and the relationship between the absorbed energy and the air pressure is shown in Figure 15.

Figure 14 shows that as the shock pressure increases, the peak stress increases, and the specimen shows an obvious strain rate effect. The dashed line in Figure 14 indicates that the stress increase in the specimen increases significantly when the air pressure reaches 0.4 MPa at 0 and 25 freeze-thaw cycles. When the air pressure reached 0.5 MPa at 50 freeze-thaw cycles, the stress increase in the specimen increased significantly, and the specimen no longer showed such a phenomenon after 75 freeze-thaw cycles. With the rise in freeze-thaw cycles, the degree of internal damage to the rubber concrete specimen increases, and the increase in impact air pressure specimen stress no longer increases.

Figure 15 shows that the absorbed energy shows an obvious strain rate effect. As the air pressure increases, the energy absorption value increases. Freeze-thaw cycles will

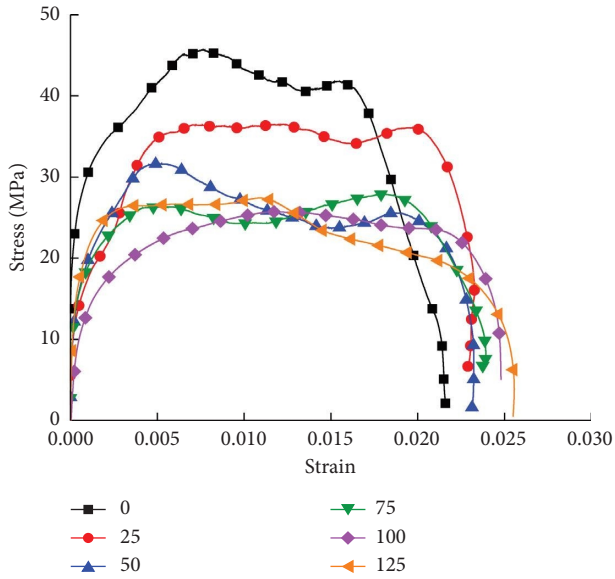

Figure 13: Stress-strain curves under freeze-thaw cycle.

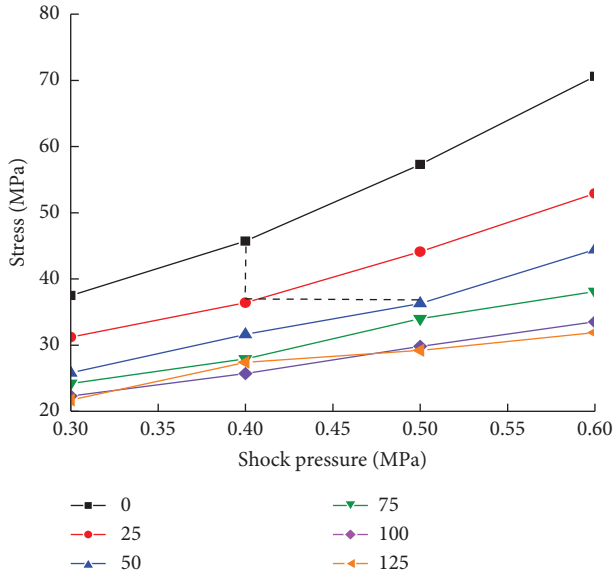

Figure 14: Relationship between impact pressure and peak stress.

reduce the energy absorption capacity of rubber concrete specimens, but this effect will gradually decrease with the increase in freeze-thaw cycles. The freeze-thaw energy absorbed by the specimens at 0.4 MPa air pressure for 25, 50, 75, 100, and 125 times decreased by 16%, 21%, 16.3%, 30.2%, and 25.7%. As the impact pressure increases, the incident energy increases, and the energy absorbed by the specimen in this process increases according to the conservation of energy. Rubber particles in concrete have a good energy absorption effect, but the rubber itself will be damaged by the freeze-thaw action, and its energy absorption effect will be reduced [27]. The rubber damage increment will no longer be obvious, and the test piece will reduce the magnitude of the change in energy absorption.

3.5. Effect of Freeze-Thaw Cycles on the Dynamic Mechanical Performance of Rubber Concrete. The effect of freeze-thaw cycles on the stress of rubber concrete under the same pressure is shown in Figure 16, and its ultimate strain and absorbed energy change law is shown in Figures 17 and 18.

Figure 16 shows that there is an obvious strain rate effect on the peak stress of the rubber concrete specimen, and the peak stress increases with the rise of the impact air pressure under the same number of freeze-thaw cycles. The peak stress of the specimens under 0 freeze-thaw cycles increased by 88.3% compared to 0.3 MPa air pressure at 0.6 MPa, while the peak stress increased by 69.6%, 72.1%, 57.4%, 50.2%, and 47.0% at 25, 50, 75, 100, and 125 freeze-thaw cycles, and the strain rate effect under freeze-thaw cycles was significantly

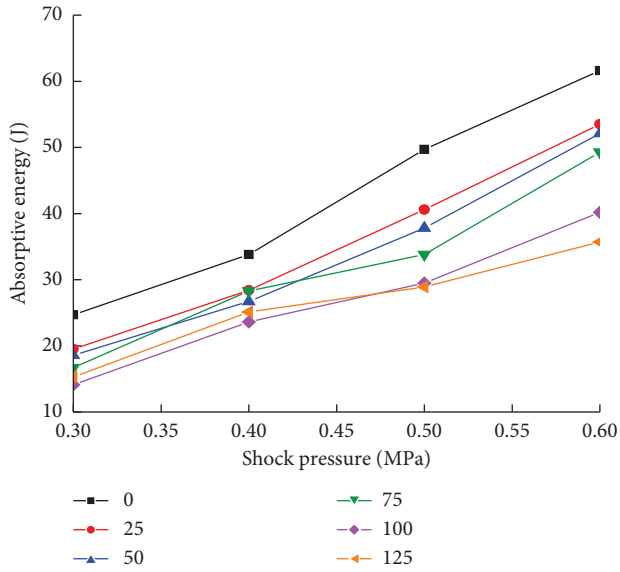

Figure 15: Relationship between shock pressure and absorbed energy.

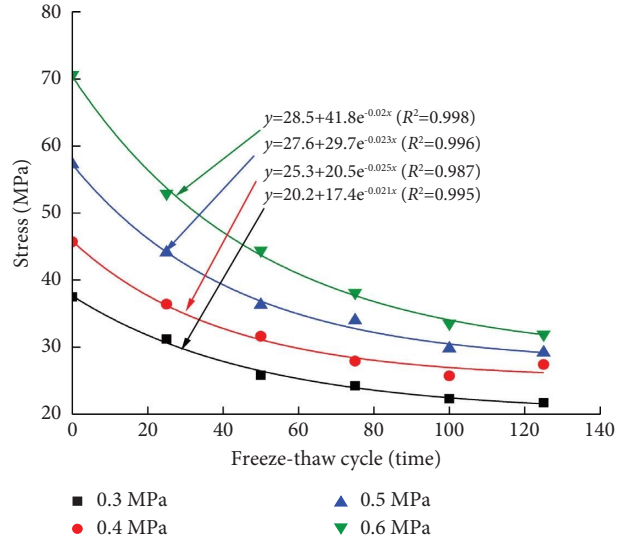

Figure 16: Relationship between the freeze-thaw cycles and peak stress.

reduced. Under the same impact pressure, the peak stress of the rubber concrete specimen decreases with the increase of the number of freeze-thaw cycles, and the two are logarithmically related. The peak stresses of the specimens were reduced by 25.1%, 37.1%, 46%, 52.5%, and 54.8% for 25, 50, 75, 100, and 125 freeze-thaw cycles under 0.6 MPa air pressure, and the stress reduction rate gradually decreased, and the stress reduction rate would no longer be obvious after the cycle times exceeded 100. Figure 17 shows that as the freeze-thaw cycles increases, the ultimate strain of the specimen increases with the same impact air pressure, and the relationship is linear. The pore water inside the specimen will produce freezing expansion during the freeze-thaw cycle, causing the expansion of pores and cracks inside the specimen, while there are differences in thermal expansion coefficients between rubber, cement, and aggregates [13]. In the process of repeated temperature differences between the three interfaces will produce stress differences, so that the expansion of primary cracks and the generation of new cracks, crack penetration between each other to increase the degree of damage to the rubber concrete, the test piece integrity is reduced, the ability to withstand external loads is weakened, the stress of the test piece under the same impact pressure is reduced, and the ultimate strain increases. With the rise of freeze-thaw cycles, the stress drop in the specimen decreases, which is due to the increase in the number of freeze-thaw cycles to rise the porosity of the specimen, the later freeze-thaw action of the pore water output of the freezing and swelling effect will no longer be obvious, the increase in the porosity of the specimen so that the temperature difference in the aggregate interface generated by

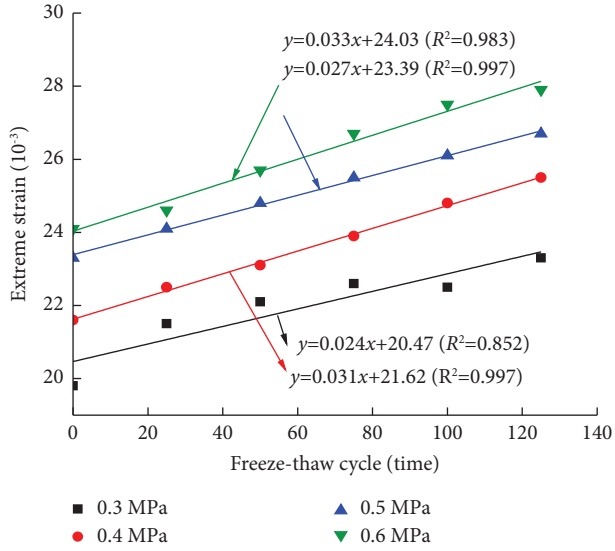

Figure 17: Relationship between the freeze-thaw cycles and ultimate strain.

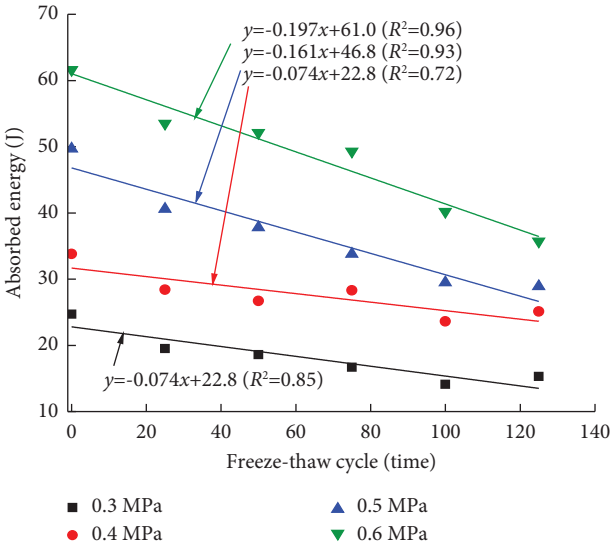

Figure 18: Relationship between the freeze-thaw cycles and absorbed energy.

the stress difference is reduced, and the specimen produces new damage to reduce the degree of stress drop.

Figure 18 shows that as freeze-thaw cycles rises, the absorbed energy of rubber concrete decreases. The absorbed energy reductions of the specimens under four different impact air pressures were 38.1%, 25.7%, 41.9%, and 42%, respectively, which were linearly related. The rubber material itself has a good energy absorption effect, and the specimen will be damaged by the concrete itself and the rubber under the action of freeze-thaw cycles, thus reducing its own energy absorption effect, and with the rise of the freeze-thaw cycles, the energy absorption energy will gradually decrease.

3.6. Effects of Shock Pressure and Freeze-Thaw Cycles on DIF. It was shown that the mechanical performance of concrete materials is improved under dynamic loading, and to further investigate the strain rate effect of rubber concrete under freeze-thaw cycles, DIF was introduced to analyze the specimens, whose value is the ratio of dynamic strength to quasi-static strength [28, 29], calculated as follows:

$$\mathrm{DIF} = \frac{f_d}{f}, \tag{5}$$

where f_d is the compressive strength, and f is the compressive strength under quasi-static load.

The variation pattern of DIF for rubber concrete under freeze-thaw cycles with different impact air pressure is shown in Figure 19.

Figure 19 shows that the specimen DIF increases with the rise of pressure, which is consistent with the results of the study on the mechanical performance of concrete in the documentation [30], where the increase of strain rate can significantly enhance the strength of the material. With the increase of the number of freeze-thaw cycles, the

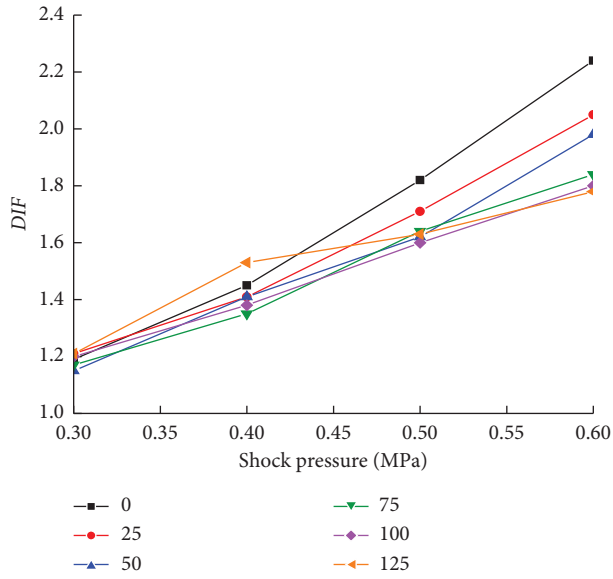

Figure 19: Relationship between impact pressure and DIF.

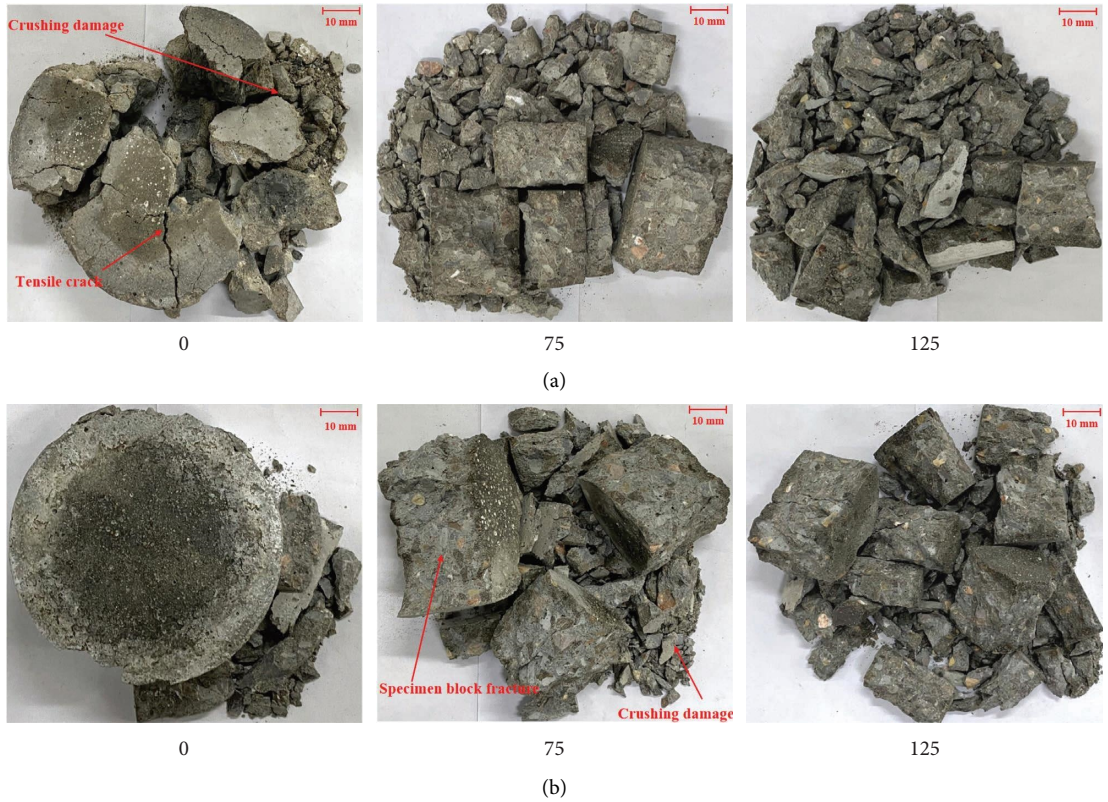

Figure 20: Specimen rupture crushing pattern. (a) Plain concrete. (b) Rubber concrete.

DIF increase of rubber concrete specimens decreased. Compared with ordinary rubber concrete, the DIF of specimens with freeze-thaw cycles at 0.6 MPa air pressure decreased by 8.5%, 11.6%, 17.9%, 19.6%, and 20.5%. Freeze-thaw cycles will weaken the strain rate effect of specimens and reduce the DIF increase of rubber concrete, and the higher the pressure, the more obvious the phenomenon. This is due to the freeze-thaw cycle, which will cause damage to the test piece, reducing its own load-bearing capacity, with the cycle number of test piece damage increases, the integrity of the lower DIF. With the increase in impact air pressure, the overall trend of increasing DIF and freeze-thaw cycle on the test piece will become more obvious.

The rupture and crushing patterns of concrete specimens with different numbers of freeze-thaw cycles under 0.4 MPa air pressure are shown in Figure 20.

Figure 20 shows that the two types of specimens coexist in split tensile and crushing damage modes under loading. With the increase in the number of freeze-thaw cycles, there is a significant increase in the degree of rupture and fragmentation of both types of concrete specimens, and the specimen rupture fragmentation decreases in size and increases in number. Freezing and thawing concrete cause damage to the concrete material itself, and the greater the number of cycles, the greater the degree of damage, the specimen's ability to withstand loading is reduced, and the degree of fragmentation increases. Comparing the rupture and crushing degrees of two kinds of concrete specimens under the same number of freeze-thaw cycles, it can be seen that the crushing degree of rubberized concrete specimens is significantly lower than that of plain concrete. The incorporation of rubber particles enhances the ductility of concrete specimens and their resistance to deformation under external loads. The rupture and crushing degree of the specimens are significantly reduced under the same impact load, and the incorporation of rubber particles enhances the deformation resistance of concrete materials.

4. Conclusions

(1) The peak stress of plain concrete under load is higher than that of rubber concrete as a whole, but its toughness and energy absorption density are significantly lower than that of rubber concrete, and the incorporation of rubber enhances the ductility and energy absorption effects of concrete materials.

(2) Freeze-thaw cycles under the action of rubber concrete longitudinal wave velocity decreases with the increase of freeze-thaw, and the degree of damage increases. The freeze-thaw action will cause fatigue damage to rubber concrete, with the increase in the number of freeze-thaw cycles test specimens wave speed decrease, and the increase in the degree of damage decreases.

(3) Freeze-thaw cycles can cause damage to the internal structure of concrete and rubber particles. The peak stress and absorbed energy decrease with the increase of freeze-thaw cycles, which are logarithmically and linearly correlated, respectively, and the ultimate strain increases with the rise of freeze-thaw cycles, which are linearly correlated.

(4) The DIF of rubber concrete under freeze-thaw cycles increased with the rise of impact air pressure, and the increase of specimen DIF decreased with the increase of freeze-thaw times, and the DIF of specimens under freeze-thaw cycles at 0.6 MPa air pressure decreased by 8.5%, 11.6%, 17.9%, 19.6%, and 20.5% compared to that of ordinary rubber concrete.

Data Availability

The data used to support the findings of the study are available from the corresponding author upon request.

Conflicts of Interest

The author declares that they have no conflicts of interest.

References

[1] F. X. Ma and Y. Liu, "Achievements, experiences and future prospects of China's automotive industry in the past 70 years," *Theoretical Exploration*, vol. 240, no. 6, pp. 108–113, 2009.

[2] M. Jang, Z. M. Kou, and S. X. Peng, "Research progress of waste rubber recovery and utilization," *China Synthetic Rubber Industry*, vol. 36, no. 3, pp. 239–243, 2013.

[3] H. W. Ge, H. X. Dong, G. R. Su, W. Q. Han, Y. Gao, and X. Y. Wang, "Research progress on resource utilization process of thermal cracking residue of waste tires," *Recyclable Resources and Circular Economy*, vol. 12, no. 10, pp. 24–27, 2019.

[4] C. S. Liu, *Study on the Durability Performance of Rubber Aggregate concrete and its Application on Bridge Deck Pavement*, Tianjin University, Tianjin, China, 2010.

[5] Y. L. Hu, P. W. Gao, F. R. Li, A. Q. Ma, and Z. P. Yu, "Experimental study on the mechanical performance of rubber concrete with different substitution rates," *Journal of Building Materials*, vol. 23, no. 1, pp. 85–92, 2020.

[6] S. S. Ki, H. Iman, and P. Kypros, "Strength and deformability of waste tyre rubber-filledreinforced concrete columns," *Construction and Building Materials*, vol. 25, no. 1, pp. 218–226, 2010.

[7] R. S. Zhao, "Experimental study on the mechanical performance of rubber concrete under impact loading," *New Building Materials*, vol. 48, no. 5, pp. 65–70, 2021.

[8] Z. L. Bai, B. X. Wang, and J. H. Lin, "Effect of freeze-thaw cycles on the bonding properties of basalt fiber woven mesh to concrete," *New Building Materials*, vol. 48, no. 9, pp. 36–40, 2021.

[9] J. Z. Zhang and X. P. Zhou, "Forecasting catastrophic rupture in brittle rocks using precursory AE time series," *Journal of Geophysical Research: Solid Earth*, vol. 125, no. 8, 2020.

[10] X. P. Zhou, Y. Niu, J. Z. Zhang, X. C. Shen, Y. Zheng, and F. Berto, "Experimental study on effects of freeze-thaw fatigue damage on the cracking behaviors of sandstone containing two unparallel fissures," *Fatigue and Fracture of Engineering Materials and Structures*, vol. 42, no. 6, pp. 1322–1340, 2019.

[11] W. Tian, K. Xing, and Y. L. Xie, "Mechanical experimental study of damage deterioration mechanism of concrete under freeze-thaw environment," *Journal of Experimental Mechanics*, vol. 30, no. 3, pp. 299–304, 2015.

[12] P. Cao, G. Peng, Q. Liu, and J. H. Xie, "Study on uniaxial dynamic mechanical performance of freeze-thaw deteriorated concrete," *Water Resources and Hydropower Engineering*, vol. 47, no. 12, pp. 105–110, 2016.

[13] T. Zhou, X. B. Xiong, and Y. Li, "Study on the effect of freeze-thaw cycles on the dynamic properties of steel fiber concrete," *Journal of Water Resources and Water Engineering*, vol. 32, no. 3, pp. 167–172+178, 2021.

[14] C. X. Wang, Z. Zhang, F. B. Cao, Y. X. Wu, C. Ye, and L. Li, "Mechanical performance and damage modeling of recycled concrete after freeze-thaw cycles," *Industrial Construction*, vol. 52, no. 5, pp. 199–207, 2022.

[15] M. T. Fan and X. Wang, "Effect of freeze-thaw cycles on the durability of rubber concrete," *Journal of Hubei University of Technology*, vol. 31, no. 4, pp. 101–104, 2016.

[16] P. T. Wu, Z. X. Liu, C. Q. Wu, H. Zhang, S. Q. Xu, and Y. Su, "Effect of steel fibers on the dynamic compression properties

of ultra-high performance concrete," *Journal of Tianjin University*, vol. 50, no. 9, pp. 939–945, 2017.

[17] J. Yu, L. Li, T. Wang et al., "Intramedullary nail versus plate treatments for distal tibial fractures: a meta-analysis," *International Journal of Surgery*, vol. 16, no. Pt A, pp. 60–68, 2015.

[18] Z. Qi, B. H. Liu, L. Yi, Z. Zeng, and Y. Zhou, "Dynamic mechanical performance of rape straw ash concrete under impact loading," *Journal of Hunan Agricultural University*, vol. 43, no. 3, pp. 336–339, 2017.

[19] X. B. Li, *Fundamentals and Applications of Rock Dynamics*, Science Press, Beijing, China, 2014.

[20] L. Song and S. S. Hu, "Two-wave and three-wave methods in SHPB data processing," *Explosion and Shock Waves*, vol. 25, no. 4, pp. 368–373, 2005.

[21] R. R. Zhang and L. W. Jing, "Analysis of the relationship between the degree of deep sandstone fragmentation and energy dissipation after high and low temperature effects in the SHPB test," *Journal of China Coal Society*, vol. 43, no. 7, pp. 1884–1892, 2018.

[22] H. Zhang, Y. W. Gao, F. Li, and F. Lu, "Dynamic mechanical performance and intrinsic modeling of polypropylene fiber concrete at high strain rates," *Journal of Central South University*, vol. 44, no. 8, pp. 3464–3473, 2013.

[23] H. B. Hu, "Experimental analysis of concrete defects detected by ultrasonic method," *Journal of Jiangsu Vocational Institute of Architectural Technology*, vol. 15, no. 2, pp. 17–20, 2015.

[24] W. J. Yao, Y. S. Liu, Y. T. Wang, and J. Y. Pang, "Performance deterioration and microstructure of rubber/concrete after salt freezing cycle," *Acta Materiae Compositae Sinica*, vol. 38, no. 12, pp. 4294–4304, 2021.

[25] M. Huang, J. M. Duan, J. X. Zhang, Q. C. Mao, J. H. Yuan, and L. T. Sun, "Fracture damage and softening principal structure relationship of basalt fiber-reinforced composite concrete under freeze-thaw cycles," *Industrial Construction*, vol. 51, no. 8, pp. 199–205+178, 2021.

[26] Z. J. Ning, *Research on Damage and Fracture of concrete under Freeze-Thaw Action*, Harbin Institute of Technology, Harbin, China, 2009.

[27] J. H. Han, Q. Yuan, L. Y. Feng, W. W. Wang, and F. Zhao, "Study of impact resistance of rubber concrete," *Yellow River*, vol. 40, no. 11, pp. 107–109+114, 2018.

[28] X. Q. Li, B. Q. Chen, Q. Du, and Z. D. Ding, "Mechanical behavior of concrete materials under high strain rates," *Journal of Yunnan University*, vol. 28, no. 5, pp. 773–783, 2016.

[29] J. K. Zhou, S. F. Wang, P. P. Qian, X. W. Shao, and Y. H. Fang, "Comparison and construction of dynamic strength improvement factor models for concrete," *Concrete*, vol. 301, no. 11, pp. 5–10, 2014.

[30] T. Yang, B. Z. Wang, and H. P. Luo, "Study of dynamic compression mechanical performance of jute fiber concrete," *Journal of Hefei University of Technology*, vol. 43, no. 8, pp. 1109–1114, 2020.